

SNUTP-00-009
nucl-th/0004055

ELECTROMAGNETIC PRODUCTION OF VECTOR MESONS AT LOW ENERGIES^a

Yongseok OH

*Center for Theoretical Physics, Seoul National University, Seoul 151-742, Korea
and*

*Institute of Physics, Academia Sinica, Nankang, Taipei, Taiwan 11529, R.O.C.
E-mail: ohys@phys.sinica.edu.tw*

Alexander I. TITOV

*Bogoliubov Laboratory of Theoretical Physics, JINR, Dubna 141980, Russia
E-mail: atitov@thsun1.jinr.ru*

T.-S. Harry LEE

*Physics Division, Argonne National Laboratory, Argonne, Illinois 60439, U.S.A.
E-mail: lee@anph09.phy.anl.gov*

We have investigated exclusive photoproduction of light vector mesons (ω , ρ and ϕ) on the nucleon at low energies. In order to explore the questions concerning the so-called missing nucleon resonances, we first establish the predictions from a model based on the Pomeron and meson exchange mechanisms. We have also explored the contributions due to the mechanisms involving s - and u -channel intermediate nucleon state. Some discrepancies found at the energies near threshold and large scattering angles suggest a possibility of using this reaction to identify the nucleon resonances.

At high energies and low momentum transfers, the exclusive electromagnetic production of vector mesons has been explained successfully by the Pomeron exchange model. [1–3] However, at low energies near threshold, meson exchange mechanisms become important, such as the π exchange in ω production and the σ exchange in ρ production. [4] Furthermore, the mechanisms involving intermediate nucleon and nucleon resonances (N^*), which could be suppressed at high energies, must also be included in a complete theoretical investigation.

To resolve the so-called “missing resonance problem”, it is essential to identify the kinematic regions where the N^* contributions are important. Many of

^aTalk at the NSTAR2000 Workshop, *The Physics of Excited Nucleons*, JLab, Newport News, Feb. 16–19, 2000

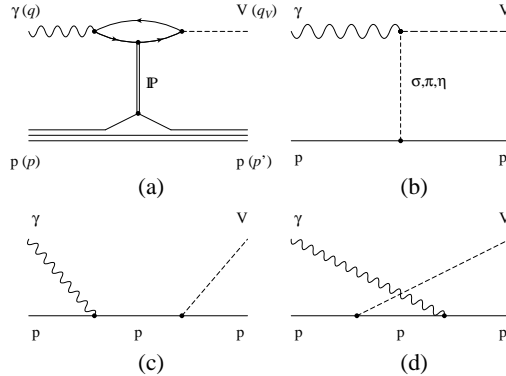


Figure 1: Three mechanisms for vector meson ($V = \rho, \omega, \phi$) photoproduction: (a) Pomeron, (b) one-boson exchange, (c) and (d) s - and u -channel intermediate nucleon diagrams.

those missing nucleon resonances are predicted to have large partial widths for their decays into channels consisting of the nucleon and a vector meson. Therefore, one may hope to find them in vector meson electromagnetic productions. There exist some reports on the contributions from the nucleon resonances in vector meson photoproduction based on quark models [5, 6] or the Regge theory [7]. However, in order to confront the forthcoming data, it is crucial to understand the non-resonant (background) production processes which could interfere strongly with the resonant production amplitudes. As a step in this direction, we have investigated the ρ , ω and ϕ photoproductions at low energies based on a model consisting of three mechanisms: Pomeron exchange, one-meson (π , η , σ) exchange and the mechanism involving an intermediate nucleon in s -channel and u -channel (called $s + u$ nucleon-term from now on).

Each of the considered production amplitude, as illustrated in Fig. 1, can be written as

$$T_{fi} = \varepsilon_{\mu}^*(V) \mathcal{M}^{\mu\nu} \varepsilon_{\nu}(\gamma), \quad (1)$$

where $\varepsilon_{\mu}(V)$ and $\varepsilon_{\nu}(\gamma)$ are the polarization vectors of the vector meson and the photon, respectively. We first consider the Pomeron exchange depicted in Fig. 1(a). In this process, the incoming photon first converts into a $q\bar{q}$ pair, which interacts with the nucleon by the Pomeron exchange before forming the outgoing vector meson. The quark-Pomeron vertex is obtained by the Pomeron-photon analogy, [1] which treats the Pomeron as a $C = +1$ isoscalar photon, as suggested by a study of nonperturbative two-gluon exchanges. [8]

	ρ	ω	ϕ
$g_{V\gamma\pi}$	0.274	0.706	0.042
$g_{V\gamma\eta}$	—	0.062	0.209

Table 1: Coupling constants $g_{V\gamma\pi}$ and $g_{V\gamma\eta}$ in unit of GeV^{-1} .

We then have [1–3, 9]

$$\begin{aligned} \mathcal{M}_P^{\mu\nu} = & i12\sqrt{4\pi\alpha_{\text{em}}}\beta_u G_P(w^2, t) F_1(t) \frac{m_V^2 \beta_f}{f_V} \frac{1}{m_V^2 - t} \left(\frac{2\mu_0^2}{2\mu_0^2 + m_V^2 - t} \right) \\ & \times \bar{u}_{m'}(p') \{ \not{q} g^{\mu\nu} - q^\mu \gamma^\nu \} u_m(p), \end{aligned} \quad (2)$$

where $\alpha_{\text{em}} = e^2/4\pi$, m and m' are the spin projections of the initial and final nucleons, respectively. Here we denote the four-momenta of the initial nucleon, final nucleon, incoming photon and outgoing vector meson by p , p' , q and q_V , respectively. Their helicities are represented by λ_p , λ'_p , λ_γ and λ_V . The Mandelstam variables are $s = W^2 = (p+q)^2$, $t = (p-p')^2$, $u = (p-q_V)^2$. The proton and vector meson masses are represented by m_p and m_V , respectively, and F_1 is the isoscalar electromagnetic form factor of the nucleon,

$$F_1(t) = \frac{4m_p^2 - 2.8t}{(4m_p^2 - t)(1 - t/0.71)^2}. \quad (3)$$

The Pomeron-exchange is described by the following Regge form,

$$G_P(w^2, t) = \left(\frac{w^2}{s_0} \right)^{\alpha_P(t)-1} \exp \left\{ -\frac{i\pi}{2} [\alpha_P(t) - 1] \right\}, \quad (4)$$

with $w^2 = (2W^2 + 2m_p^2 - m_V^2)/4$ and $s_0 = 1/\alpha'_P$. The Pomeron trajectory is taken to be the usual form $\alpha_P(t) = 1.08 + \alpha'_P t$ with $\alpha'_P = 0.25 \text{ GeV}^{-2}$. In Eq. (2), f_V is the vector meson decay constant: $f_\rho = 5.04$, $f_\omega = 17.05$ and $f_\phi = 13.13$. The coupling constants $\beta_u = \beta_d = 2.07 \text{ GeV}^{-1}$, $\beta_s = 1.60 \text{ GeV}^{-1}$ and $\mu_0^2 = 1.1 \text{ GeV}^2$ are chosen to reproduce the total cross section data at high energies $E_\gamma \geq 10 \text{ GeV}$ where the vector meson photoproductions are completely dominated by Pomeron-exchange.

For the one-meson exchange diagram of Fig. 1(b), we consider scalar and pseudoscalar meson exchanges. The vector meson exchange is not allowed in this process and the possible exchange of axial vector mesons [10] is suppressed at low energies mainly because of their heavy masses and small coupling constants.

The pseudoscalar meson exchange amplitude can be obtained from the Lagrangian,

$$\mathcal{L}_\varphi = g_{V\gamma\varphi}\epsilon^{\mu\nu\alpha\beta}\partial_\mu V_\nu\partial_\alpha A_\beta\varphi - ig_{\varphi NN}\bar{N}\gamma_5\varphi N, \quad (5)$$

where $\varphi = (\pi^0, \eta)$ and A_μ is the photon field. The coupling constants $g_{V\gamma\pi}$ and $g_{V\gamma\eta}$, as given in Table 1, are obtained from the experimental partial widths [11] of the vector meson radiative decays $V \rightarrow \gamma\varphi$. We use $g_{\pi NN}^2/4\pi = 14.0$ and the SU(3) relation to obtain $g_{\eta NN}/g_{\pi NN} \simeq 0.35$. To account for the effects due to the finite hadron size at each vertex, the resulting Feynman amplitudes are regularized by the following form factors,

$$F_{\varphi NN} = \frac{\Lambda_\varphi^2 - M_\varphi^2}{\Lambda_\varphi^2 - t}, \quad F_{V\gamma\varphi} = \frac{\Lambda_{V\gamma\varphi}^2 - M_\varphi^2}{\Lambda_{V\gamma\varphi}^2 - t}, \quad (6)$$

where ($\Lambda_\pi = 0.7$, $\Lambda_{V\gamma\pi} = 0.77$) and ($\Lambda_\eta = 1.0$, $\Lambda_{V\gamma\eta} = 0.9$) in GeV unit. [12]

The scalar (σ) meson exchange was introduced in Ref. [4] to describe the ρ photoproduction. This can be considered as an effective way to account for the two- π exchange in ρ production, which is expected to be significant because of the large branching ratio of $\rho \rightarrow \pi^+\pi^-\gamma$ decay. The contribution from the σ exchange can be obtained from the following Lagrangian,

$$\mathcal{L}_\sigma = \frac{eg_{V\gamma\sigma}}{M_V}(\partial^\mu V^\nu\partial_\mu A_\nu - \partial^\mu V^\nu\partial_\nu A_\mu)\sigma + g_{\sigma NN}\bar{N}N\sigma. \quad (7)$$

We also regularize the resulting one-meson-exchange amplitude by the form factors,

$$F_{\sigma NN} = \frac{\Lambda_\sigma^2 - M_\sigma^2}{\Lambda_\sigma^2 - t}, \quad F_{V\gamma\sigma} = \frac{\Lambda_{V\gamma\sigma}^2 - M_\sigma^2}{\Lambda_{V\gamma\sigma}^2 - t}. \quad (8)$$

Following Ref. [4], we use $M_\sigma = 0.5$ GeV, $g_{\sigma NN}^2/4\pi = 8.0$, $\Lambda_\sigma = 1.0$ GeV and $\Lambda_{V\gamma\sigma} = 0.9$ GeV. The coupling constant $g_{V\gamma\sigma}$ is around 3.0 for reproducing the total cross sections of ρ photoproduction near threshold. We do not consider the σ -exchange in ω and ϕ photoproductions, since the radiative decays of these two vector mesons into $\pi^+\pi^-$ states are much weaker than that into single pion state. This could be understood by considering the current-field identity. [4] (See also Ref. [12].)

Finally we consider the $s + u$ nucleon-term shown in Fig. 1(c,d). The corresponding amplitudes can be obtained from the following Lagrangian,

$$\mathcal{L}_N = g_{VNN}\bar{N}\left[\gamma_\mu V^\mu - \frac{\kappa_V}{2M_N}\sigma_{\mu\nu}\partial^\nu V^\mu\right]N - e\bar{N}\left[\gamma_\mu A^\mu - \frac{\kappa_p}{2M_N}\sigma_{\mu\nu}\partial^\nu A^\mu\right]N, \quad (9)$$

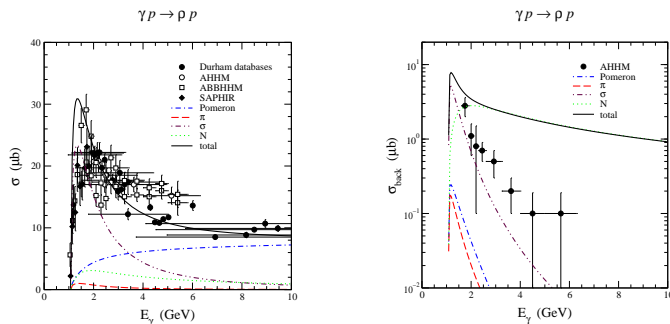


Figure 2: (Left figure) total cross section of ρ photoproduction. The dot-dashed, dashed, dot-dot-dashed, dotted and solid lines are Pomeron exchange, π exchange, σ exchange, intermediate nucleon and the sum of the amplitudes, respectively. The experimental data are from Refs. [15–18]. (Right figure) cross section σ_{back} with the data from Ref. [16].

where the anomalous magnetic moment of the proton is $\kappa_p = 1.79$. The coupling constants are chosen to be $(g_{\rho NN}, \kappa_\rho) = (6.2, 2.0)$ and $(g_{\omega NN}, \kappa_\omega) = (7.0, 0)$, as determined in a study of πN scattering and pion photoproduction. [13] In this study, we do not consider the $s + u$ nucleon-term in ϕ photoproduction by assuming $g_{\phi NN} \approx 0$ due to the OZI rule. A possible modification due to nonvanishing ϕNN coupling can be found in Ref. [12]. The form factor F_V for VNN vertex is assumed to be of the form given by Ref. [14],

$$F_V(s, u) = \frac{1}{2} \left(\frac{\Lambda_{VNN}^4}{\Lambda_{VNN}^4 + (s - M_N^2)^2} + \frac{\Lambda_{VNN}^4}{\Lambda_{VNN}^4 + (u - M_N^2)^2} \right), \quad (10)$$

with $\Lambda_{VNN} = 0.8$ GeV.

With the production amplitudes given above, we have explored the extent to which the existing data of vector meson photoproductions can be described by the non-resonant (background) mechanisms. The ρ photoproduction cross sections are calculated from the amplitudes due to Pomeron, π , σ exchanges and the $s + u$ nucleon-term. In the left panel of Fig. 2 we show that the calculated total cross sections (solid curve) agree to a very large extent with the data up to $E_\gamma = 10$ GeV. The important role of the σ exchange (dot-dot-dashed curve) at energies near threshold is also shown there. The dynamical content of our model can be better seen by investigating angular distributions. For example, given in the right panel of Fig. 2 is the backward integrated cross sections defined by

$$\sigma_{\text{back}} \equiv \int_{\pi/2}^{\pi} \frac{d\sigma}{d\theta} d\theta. \quad (11)$$

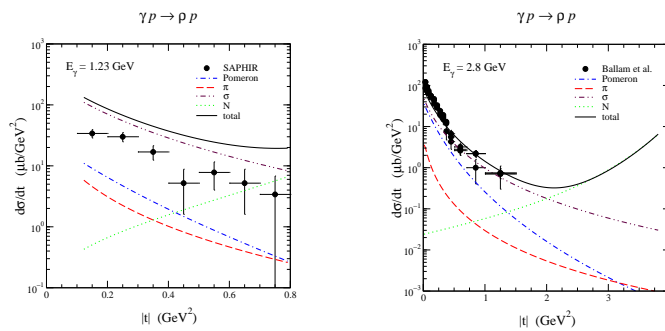


Figure 3: Differential cross sections of ρ photoproduction at $E_\gamma = 1.23$ and 2.8 GeV. The experimental data are from Refs. [18,19]. Notations are the same as in Fig. 2.

The predicted backward cross sections (solid curve) clearly overestimate the experimental data. We find that this is caused by the dominant contributions (dotted curve) from the $s+u$ nucleon-term. On the other hand, the calculated cross sections will be too low if these mechanisms involving an intermediate nucleon state are not included in the calculation. This suggests that some other production mechanisms, which can give important contributions at large scattering angles, must be included in a more complete model. This can also be seen in the angular distributions of the differential cross sections shown in Fig. 3. We see that the contribution from the $s+u$ nucleon-term (dotted curves) become dominant at large scattering angles. Therefore, precise measurements of the differential cross sections in the backward scattering region will shed light on the role of the intermediate nucleon states. At very low energies near threshold, $E_\gamma \leq 2$ GeV, our predictions overestimate significantly the data. This is perhaps mainly due to the neglect of the N^* excitations in our calculations.

The ω photoproduction cross sections are calculated from the Pomeron, π and η exchanges and the $s+u$ nucleon-term. The predicted total and differential cross sections are compared with the data in Fig. 4. We see that the one-pion exchange (long dashed curves) dominates ω photoproduction up to $E_\gamma \approx 6$ GeV. The predicted total cross sections somewhat underestimate the recent SAPHIR data in the $E_\gamma \leq 2$ GeV region where the mechanisms involving the excitation of nucleon resonances are expected to play some roles. Similar to the case of ρ photoproduction, the $s+u$ nucleon-term also dominates the cross sections at large $|t|$ region.

For ϕ photoproduction, we consider the Pomeron and pseudoscalar meson exchanges only. We refer the calculations on the scalar meson exchanges and

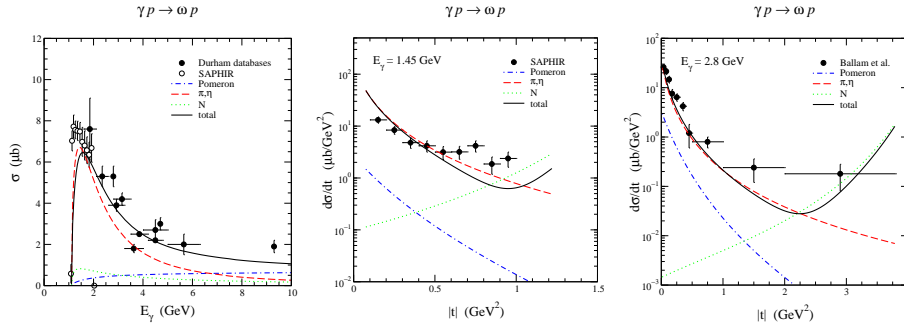


Figure 4: Total and differential cross sections of ω photoproduction. The experimental data are from Refs. [15, 18, 19]. Notations are the same as in Fig. 2.

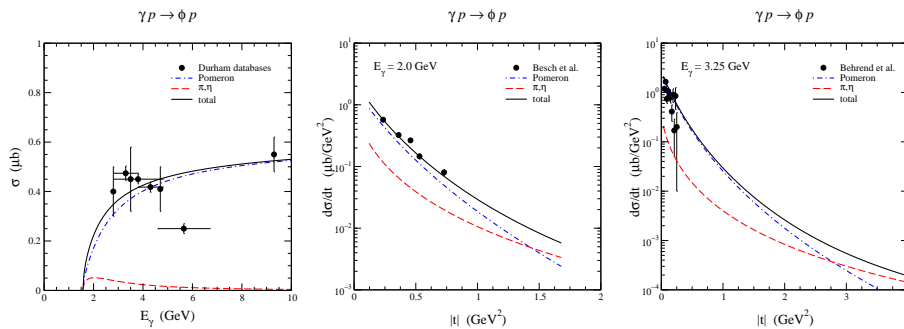


Figure 5: Total and differential cross sections of ϕ photoproduction. The experimental data are from Refs. [15, 21, 22]. Notations are the same as in Fig. 2.

direct ϕ radiation arising from the non-vanishing ϕNN coupling to Ref. [12] and the effects of nonvanishing strangeness of the nucleon to Refs. [9, 20]. In Fig. 5 we show that the predicted total and differential cross sections agree well with the very limited data. Contrary to the cases of ρ and ω photoproductions, the Pomeron exchange (dash-dotted curves) gives the major contribution to the total cross section even at energies near threshold. This is mainly due to the fact that the coupling of ϕ to the nucleon is suppressed by the OZI rule. The contributions from π and η exchanges are also found to be small. Therefore ϕ photoproduction can provide a useful tool to study the nature of the Pomeron exchange.

In summary, we have investigated the exclusive photoproduction of light vector mesons (ρ , ω and ϕ) at low energies. Our model includes the Pomeron exchange, meson (π , η , σ) exchange and the s - and u -channel nucleon terms.

It is found that the predicted cross sections agree with the existing data to a large extent. However, some significant discrepancies are found in the total and differential cross sections at low energies and at large scattering angles. It is possible that such discrepancies could be removed by extending our model to include the effects due to the excitation of nucleon resonances. Our investigation in this direction is in progress, aiming at using the new data from current experimental facilities to test various QCD-inspired models of hadron structure.

Acknowledgments

We are grateful to V. Burkert, W.-C. Chang, F. J. Klein, N. I. Kochelev and T. Nakano for fruitful discussions and informations. Y.O. thanks the Theory Division of Argonne National Laboratory and the organizer of this workshop for the warm hospitality and financial support. This work was supported in part by KOSEF of Korea, NSC of Republic of China, Russian Foundation for Basic Research under Grant No 96-15-96426 and U.S. DOE Nuclear Physics Division Contract No. W-31-109-ENG-38.

References

1. A. Donnachie and P. V. Landshoff, Nucl. Phys. B **244**, 322 (1984); Nucl. Phys. B **267**, 690 (1986); Phys. Lett. B **185**, 403 (1987).
2. J.-M. Laget and R. Mendez-Galain, Nucl. Phys. A **581**, 397 (1995).
3. M. A. Pichowsky and T.-S. H. Lee, Phys. Rev. D **56**, 1644 (1997).
4. B. Friman and M. Soyeur, Nucl. Phys. A **600**, 477 (1996).
5. Q. Zhao, Z. Li and C. Bennhold, Phys. Rev. C **58**, 2393 (1998).
6. Q. Zhao *et al.*, Nucl. Phys. A **660**, 323 (1999).
7. J. M. Laget, Saclay Report (2000), hep-ph/0003213.
8. P. V. Landshoff and O. Nachtmann, Z. Phys. C **35**, 405 (1987).
9. A. I. Titov *et al.*, Phys. Rev. C **58**, 2429 (1998).
10. N. I. Kochelev *et al.*, Phys. Rev. D **61**, 094008 (2000).
11. Particle Data Group, C. Caso *et al.*, Eur. Phys. J. C **3**, 1 (1998).
12. A. I. Titov *et al.*, Phys. Rev. C **60**, 035205 (1999).
13. T. Sato and T.-S. H. Lee, Phys. Rev. C **54**, 2660 (1996).
14. H. Habermann *et al.*, Phys. Rev. C **58**, 40 (1998).
15. The Durham RAL Databases, <http://durpdg.dur.ac.uk/hepdata>.
16. AHHM Collab., W. Struczinski *et al.*, Nucl. Phys. B **108**, 45 (1976).
17. ABBHHM Collab., R. Erbe *et al.*, Phys. Rev. **175**, 1669 (1968).
18. SAPHIR Collab., F. J. Klein *et al.*, π N Newslett. **14**, 141 (1998); F. J. Klein, Ph.D. thesis, Bonn Univ. (1996),

19. J. Ballam *et al.*, Phys. Rev. D **5**, 545 (1972); Phys. Rev. D **7**, 3150 (1973).
20. A. I. Titov, Y. Oh and S. N. Yang, Phys. Rev. Lett. **79**, 1634 (1997); Y. Oh *et al.*, Phys. Lett. B **462**, 23 (1999).
21. H. J. Besch *et al.*, Nucl. Phys. B **70**, 257 (1974).
22. H.-J. Behrend *et al.*, Nucl. Phys. B **144**, 22 (1978).